Limits on inelastic dark matter from ZEPLIN-III

D. Yu. Akimov,[1] H. M. Araújo,[2] E. J. Barnes,[3] V. A. Belov,[1] A. Bewick,[2] A. A. Burenkov,[1] R. Cashmore,[4] V. Chepel,[5] A. Currie*,[2] D. Davidge,[2] J. Dawson,[2] T. Durkin,[6] B. Edwards,[6] C. Ghag,[3] A. Hollingsworth,[3] M. Horn,[2] A. S. Howard,[2] A. J. Hughes,[6] W. G. Jones,[2] G. E. Kalmus,[6] A. S. Kobyakin,[1] A. G. Kovalenko,[1] V. N. Lebedenko,[2] A. Lindote,[5,6] I. Liubarsky,[2] M. I. Lopes,[5] R. Lüscher,[6] K. Lyons,[2] P. Majewski,[6] A. StJ. Murphy,[3] F. Neves,[5,2] S. M. Paling,[6] J. Pinto da Cunha,[5] R. Preece,[6] J. J. Quenby,[2] L. Reichhart,[3] P. R. Scovell,[3] C. Silva,[5] V. N. Solovov,[5] N. J. T. Smith,[6] P. F. Smith,[6] V. N. Stekhanov,[1] T. J. Sumner,[2] C. Thorne,[2] L. de Viveiros,[5] and R. J. Walker[2]

(ZEPLIN-III)

[1] *Institute for Theoretical and Experimental Physics, Moscow, Russia*
[2] *Blackett Laboratory, Imperial College London, UK*
[3] *School of Physics and Astronomy, University of Edinburgh, UK*
[4] *Brasenose College, University of Oxford, UK*
[5] *LIP–Coimbra & Department of Physics of the University of Coimbra, Portugal*
[6] *Particle Physics Department, Rutherford Appleton Laboratory, Chilton, UK*

(Dated: April 2, 2010)

We present limits on the WIMP-nucleon cross section for inelastic dark matter derived from the 2008 run of ZEPLIN-III. Cuts, notably on scintillation pulse shape and scintillation-to-ionisation ratio, give a net exposure of 63 kg · days in the range 20–80 keV nuclear recoil energy, in which 6 events are observed. Upper limits on signal rate are derived from the maximum empty patch in the data. Under standard halo assumptions a small region of parameter space consistent, at 99% CL, with causing the 1.17 ton · year DAMA modulation signal is allowed at 90% CL: it is in the mass range 45–60 GeV c^{-2} with a minimum CL of 88%, again derived from the maximum patch. This is the tightest constraint on that explanation of the DAMA result yet presented using a xenon target.

PACS numbers: 95.35.+d, 29.40.Mc, 29.40.Gx

Dark matter in the form of weakly interacting massive particles (WIMPs) which scatter predominantly into a higher-mass state has been proposed [1] as an explanation of the annually modulated event rate in DAMA/NaI and DAMA/LIBRA [2] which is also consistent with the upper limits on WIMP-nucleon elastic scattering rates from other experiments [3–5]. In such inelastic dark matter (iDM) models, scattering with energy transfer E_{R} due to a WIMP of ground state mass m_χ and mass change δ requires a minimum relative speed

$$v_{\mathrm{min}} = \frac{1}{\sqrt{2 m_{\mathrm{N}} E_{\mathrm{R}}}} \left(\frac{m_{\mathrm{N}} E_{\mathrm{R}}}{\mu_{\mathrm{N}}} + \delta \right), \tag{1}$$

where m_{N} is the nucleus mass and μ_{N} is the reduced mass of the WIMP-nucleus system. A non-zero δ results in a recoil spectrum that is zero at low energy and more sensitive, compared with elastic scattering, to the upper tail of the WIMP velocity distribution. WIMPs with velocity below $(2\delta/\mu_{\mathrm{N}})^{0.5}$ will not scatter inelastically at all and so, for a given local escape velocity, more m_χ-δ parameter space is accessible to heavier target nuclei. However, systematic uncertainty in the expected relative rates in different targets due to nuclear form factors and WIMP velocity distributions grows with the difference in atomic mass [6]. On balance, xenon is well suited to test iDM models that would, by predicting a modulated rate of scattering against iodine nuclei, explain the DAMA observation.

ZEPLIN-III (described in detail in Refs. [7, 8]) is a liquid/gas detector designed to search for WIMPs scattering against xenon nuclei in the 6.5 kg fiducial liquid volume. It is built of low-radionuclide components, encased in hydrocarbon and lead shielding, and operated in the Palmer Laboratory at Boulby Mine beneath 2850 m water-equivalent rock overburden. Events are characterised by two light signals recorded by an array of 31 photomultiplier tubes (PMTs). The summed scintillation signal from the liquid is denoted by $S1$. A 3.9 kV cm^{-1} electric field in the liquid extracts ionisation charge from the interaction site, drifts it to the surface and forces emission into the gas layer above; there, an electroluminescence signal, $S2$, is produced. As described in Ref. [4], events with one $S1$ and one $S2$ signal were selected and cuts made, based on the pattern of light distribution, to remove multiple-scintillation, single-ionisation events.

An event's electron recoil equivalent energy, denoted by E_{ee} and measured in keVee, is derived from the pulse area of the $S1$ signal, normalised to 122 keV photoabsorption using a ^{57}Co γ-ray source. Discrimination between nuclear and electron recoil events is achieved primarily through the ratio of scintillation and ionisation signals. Additional discrimination has been achieved here

*Corresponding author, email: alastair.currie08@imperial.ac.uk

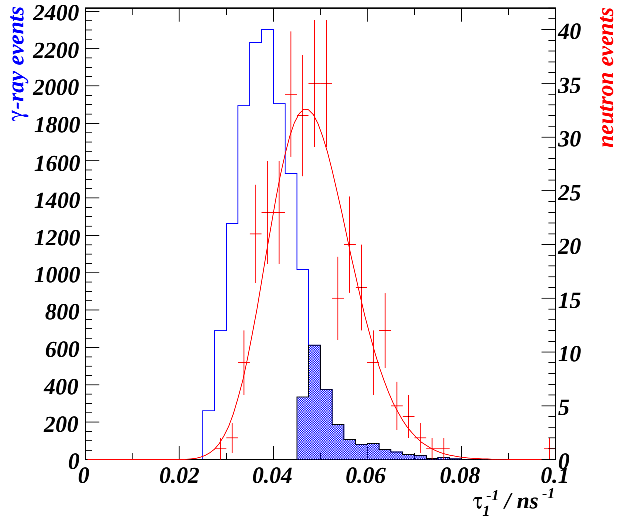

Figure 1: The effect of the τ_1 cut on the 20–25 keVee bin, over all $S2/S1$. The points and right scale correspond to AmBe data, fitted by a gamma distribution. The outlined histogram and left scale correspond to ^{137}Cs data before the cut with a shaded region corresponding to the 13% of electron recoil events which are not rejected by the cut.

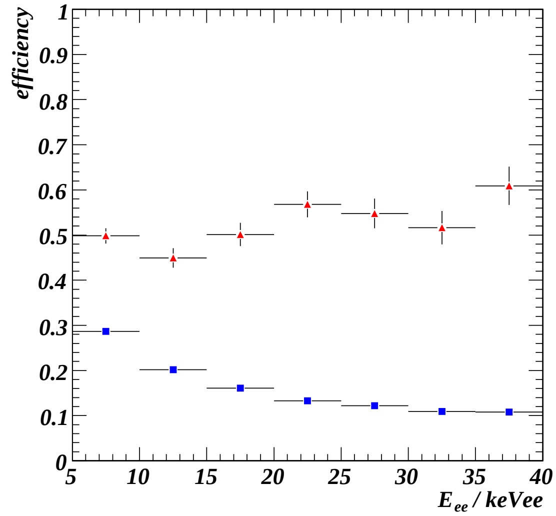

Figure 2: The efficiency of the τ_1 cut on calibration events over all $S2/S1$, for energy bins 5–40 keVee. Red triangles are AmBe data and blue squares are ^{137}Cs data.

using scintillation pulse shape. Recoiling electrons and nuclei produce different proportions of the singlet and triplet excited dimer states, which have lifetimes of 4 and 22 ns respectively [9]. PMT traces are sampled at 2 ns intervals and so the mean arrival time of the $S1$ pulse area, denoted by τ_1, is a useful discriminator. The timing of AmBe neutron calibration events within each 5-keVee bin from 5 to 40 keVee is well described by gamma distributions in $1/\tau_1$ [10]. Fitting a polynomial in $E_{\rm ee}$ to the medians of the gamma distributions produces a cut on τ_1 with 50% signal acceptance. Fig. 1 shows the separation of the two recoil types and the effect of the cut in an example bin. The power of the timing cut to reduce electron recoil background increases with energy, as seen in Fig. 2, mainly due to a narrowing in the τ_1 distribution of electron recoil events.

AmBe calibration data were also used to obtain the $S2/S1$ distribution of elastic nuclear recoil events which pass the timing cut, as a function of $E_{\rm ee}$. As in Ref. [4], the $\log_{10}(S2/S1)$ distribution was fitted by a Gaussian in each energy bin, and the energy dependence of the fitted means and standard deviations parametrised by a power law to define a cut with 47.7% signal acceptance. Charge recombination causes $S2$ and $S1$ to be microscopically anticorrelated at a given energy; in principle, therefore, the $S2/S1$ distribution has some dependence on the recoil energy spectrum. However, the low level of field-induced $S1$ suppression observed for nuclear recoils in xenon [11] suggests that the effect is relatively small. Here we have assumed, as xenon experiments historically have, that the $S2/S1$ distribution at fixed $S1$ for neutron calibration events is an adequate approximation to that for signal events. After efficiencies from dead time, pulse-finding, event reconstruction and the cuts on $S2/S1$ and τ_1, the net exposure for signal events is 63 kg $\cdot$ days, with 5% uncertainty due to neutron calibration statistics.

Nuclear recoil-equivalent energy, $E_{\rm R}$, is determined as in Ref. [4] from $E_{\rm ee}$ via a conversion factor:

$$E_{\rm R} = \frac{S_{\rm e}}{L_{\rm eff} S_{\rm n}} E_{\rm ee}, \quad (2)$$

where $S_{\rm e}$ and $S_{\rm n}$ are the field-induced suppression factors for the light yield of electron and nuclear recoils and $L_{\rm eff}$ is the zero-field light yield of nuclear recoils relative to that of electron recoils. An energy range of 20–80 keV nuclear recoil energy (8.4–38.3 keVee) was chosen to include the majority of events predicted by the quenched, inelastic WIMP-iodine scattering interpretation of the DAMA modulation [12].

Fig. 3 shows the six search events which passed all cuts. The combined efficiency of the cuts on $S2/S1$ and τ_1 for search data (6 in 1.3×10^5) is no higher than for electron-recoil calibration data (7 in 8.5×10^4), suggesting that the surviving search events may well constitute the tail of the electron-recoil background population. Without the timing cut the box would have contained 27 events.

For WIMPs which couple equally to protons and neutrons, the differential rate for spin-independent WIMP-nucleus scattering in a target of total mass $M_{\rm T}$ is given

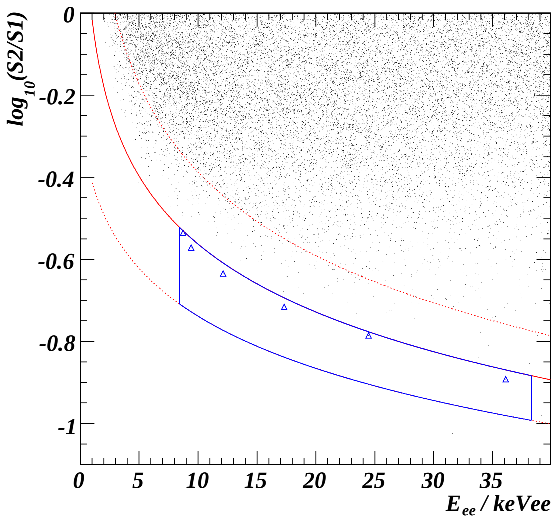

Figure 3: Search data passing all cuts except those on $E_{\rm ee}$ and $S2/S1$. Events passing all cuts are highlighted by triangles. The solid and dashed lines show the mean plus and minus two standard deviations for elastic AmBe calibration events, and the vertical lines indicate 20–80 keV nuclear recoil equivalent energy.

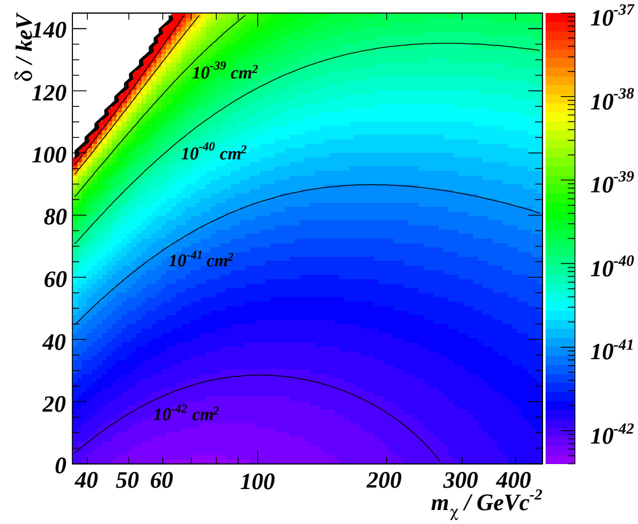

Figure 4: (color online) 90% limit on σ_n/cm^2 as a funciton of mass and splitting. The upper left region predicts no inelastic scattering during the run.

by:

$$\frac{dR}{dE_{\rm R}}\left(E_{\rm R},t\right)=\frac{M_{\rm T}\rho_\chi\sigma_n}{2m_\chi\mu_{\rm n}^2}A^2F^2(q)\int_{\rm v_{min}}^{\infty}d^3v\frac{f\left(\vec{v},t\right)}{v}, \quad (3)$$

where ρ_χ is the local WIMP density, A is the atomic number of the target nucleus, σ_n is the WIMP-nucleon cross section, $\mu_{\rm n}$ is the WIMP-nucleon reduced mass and $f\left(\vec{v},t\right)$ is the WIMP velocity distribution in the target frame. A Helm form factor was used:

$$F(q)=\frac{3j_1\left(qr_n\right)}{qr_n}\exp\left(-(qs)^2/2\right), \quad (4)$$

for momentum transfer q, where the effective nuclear radius is taken to be $r_n=\sqrt{1.44A^{\frac{2}{3}}-5}$ fm, the skin depth $s=1$ fm and j_1 is a spherical Bessel function.

Recoil energy spectra were calculated under a standard halo model: $\rho_\chi=0.3\ \mathrm{GeV\,c^{-2}\,cm^{-3}}$, a Maxwellian velocity distribution with $v_0=220\ \mathrm{m\,s^{-1}}$ truncated at escape velocity $v_{\rm esc}$ in the galactic frame, and an Earth velocity parametrised as in Ref. [13]. The underlying spectrum for given m_χ, δ and σ_n was modified by the energy resolution and efficiency of ZEPLIN-III and then averaged over the 83-day run to produce a signal model. The energy resolution, dominated by Poisson statistics of photoelectron production and the variance of the single-photoelectron response, is $\sigma/E_{\rm R}=1.5\left(E_{\rm R}/\mathrm{keV}\right)^{-0.5}$.

The maximum patch statistic [14] was used to derive single-sided upper limits on the rate of signal events in the 20–80 keV range. No background estimate is used; consequently, the null hypothesis cannot be ruled out by this method. Events were mapped onto a plane of uniform signal density by integrating the signal spectrum in $E_{\rm R}$ and the fitted profile in $S2/S1$. For models in the previously un-excluded region of iDM parameter space, the largest empty rectangle in the re-mapped search box has a fractional acceptance of 0.73–0.75; this implies a 90% CL limit of 5.4–5.1 expected signal events in the box. The resultant limits on σ_n for $v_{\rm esc}=550\ \mathrm{km\,s^{-1}}$ are plotted in Fig. 4.

Signal modulation spectra for the combined DAMA experiments were constructed with resolution as described in Refs. [15, 16] and parametrised in Ref. [17]. An iodine quenching factor of 0.08 [18, 19] was used; the exclusion results are relatively insensitive to channelling effects [20] which are, conservatively, omitted. The parameters m_χ, δ and σ_n were fitted, by minimizing χ^2, to the observed modulation amplitude in 0.5-keVee bins from 2–10 keVee and a single 10–20 keVee bin, following Ref. [17]. A 90% confidence interval for the local escape velocity from Ref. [21] is 498–608 km s^{-1} and the cross section excluded by ZEPLIN-III depends on the true $v_{\rm esc}$. Non-Maxwellian velocity distributions would cause a similar systematic effect. Fig. 5 shows the ZEPLIN-III constraints on parameter space consistent with causing the DAMA modulation for three values of $v_{\rm esc}$. DAMA-explaining cross sections are excluded at the 88% confidence level. Fluctuations of $\pm1\cdot\sigma$ in the cut efficiencies derived from neutron calibration would change this minimum CL within the range 87–90%.

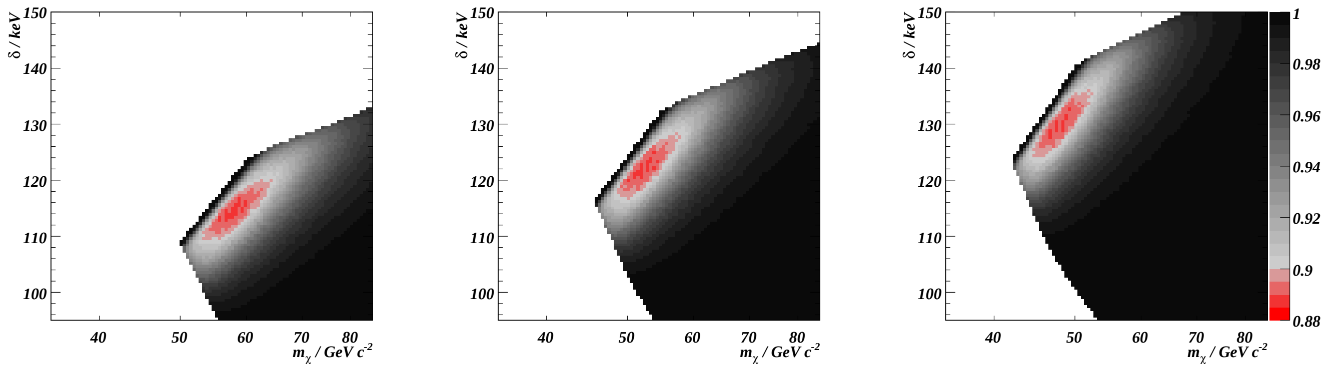

Figure 5: In m_χ–δ space, the confidence level at which ZEPLIN-III excludes the lowest value of σ_n consistent, at 99% CL, with causing the DAMA modulation. Three values of $v_{\rm esc}$ are shown: (from left) 500, 550 and 600 km s^{-1}.

In summary, a search of 63 kg · days net exposure with a xenon target yielded 6 candidate events in the range 20–80 keV nuclear recoil equivalent energy. They were consistent, both in number and scintillation-to-ionisation ratio, with belonging to the tail of an electron recoil background population. Single-sided upper limits were set on the WIMP-nucleon cross section, constraining the DAMA-explaining region of iDM parameter space: for a standard halo model there remains a 90% CL allowed region for WIMP masses in the range 45–60 GeV c^{-2}, with minimum CL 88%. This is more stringent than limits from other xenon and germanium experiments [5, 22, 23] and supports previous exclusions [17] based on CRESST-II data. In particular, a target element of similar mass to iodine reduces systematic uncertainty due to the WIMP velocity distribution.

The UK groups acknowledge the support of the Science & Technology Facilities Council for the ZEPLIN-III project and for maintenance and operation of the underground Palmer laboratory which is hosted by Cleveland Potash Ltd at Boulby Mine. The project would not be possible without the cooperation of the management and staff of CPL. The authors thank Neal Weiner for helpful discussions. We acknowledge support from a Joint International Project award, held at ITEP and ICL, from the Russian Foundation of Basic Research (08-02-91851 KO a) and the Royal Society. LIP-Coimbra acknowledges financial support from Fundação para Ciência e Tecnologia through the project grants CERN/FP/83501/2008 and CERN/FP/109320/2009, as well as postdoctoral grants SFRH/BPD/27054/2006 and SFRH/BPD/47320/2008. This work was supported in part by SC Rosatom; by Russian Grant SS-1329.2008.2 and by the Russian Ministry of Education and Science contract 02.740.11.0239. The University of Edinburgh is a charitable body, registered in Scotland, with the registration number SC005336.

[1] D. Tucker-Smith and N. Weiner, Phys. Rev. D **64**, 043502 (2001).
[2] R. Bernabei et al., Eur. Phys. J. C (2010), doi: 10.1140/epjc/s10052-010-1303-9.
[3] J. Angle et al., Phys. Rev. Lett. **100**, 021303 (2008).
[4] V. N. Lebedenko et al., Phys. Rev. D **80**, 052010 (2009).
[5] Z. Ahmed et al. (2009), arXiv:0912.3592v1.
[6] M. Kuhlen et al., JCAP **02**, 030 (2010).
[7] D. Y. Akimov et al., Astroparticle Phys. **27**, 46 (2007).
[8] H. M. Araujo et al., Astroparticle Phys. **26**, 140 (2006).
[9] A. Hitachi et al., Phys. Rev. B **27**, 5279 (1983).
[10] G. Alner et al., Astroparticle Physics **23**, 444 (2005).
[11] A. Manzur et al., Phys. Rev. C **81**, 025808 (2010).
[12] S. Chang et al., Phys. Rev. D **79**, 043513 (2009).
[13] G. Gelmini and P. Gondolo, Phys. Rev. D **64**, 023504 (2001).
[14] S. Henderson et al., Phys. Rev. D **78**, 015020 (2008).
[15] R. Bernabei et al., Il Nuovo Cimento A **112**, 545 (1999).
[16] R. Bernabei et al., Eur. Phys. J. C **53**, 205 (2008).
[17] K. Schmidt-Hoberg and M. W. Winkler, JCAP **09**, 010 (2009).
[18] G. Gerbier et al., Astroparticle Physics **11**, 287 (1999).
[19] D. Tovey et al., Physics Letters B **433**, 150 (1998).
[20] R. Bernabei et al., Nucl. Instrum. Meth. A **592**, 297 (2008).
[21] M. C. Smith et al., Mon. Not. Roy. Astron. Soc. **379**, 755 (2007).
[22] D. B. Cline et al. (2009), arXiv:0906.4119v3.
[23] J. Angle et al., Phys. Rev. D **80**, 115005 (2009).